Critical viscosity exponent for classical fluids

Hong Hao, Richard A. Ferrell, and Jayanta K. Bhattacharjee*
Department of Physics, University of Maryland, College Park, Maryland 20742, USA
(Received 23 April 2004; revised manuscript received 9 November 2004; published 14 February 2005)

A self-consistent mode-coupling calculation of the critical viscosity exponent z_η for classical fluids is performed by including the memory effect and the vertex corrections. The incorporation of the memory effect is through a self-consistency procedure that evaluates the order parameter and shear momentum relaxation rates at nonzero frequencies, thereby taking their frequency dependence into account. This approach offers considerable simplification and efficiency in the calculation. The vertex corrections are also demonstrated to have significant effects on the numerical value for the critical viscosity exponent, in contrast to some previous theoretical work which indicated that the vertex corrections tend to cancel out from the final result. By carrying out all of the integrations analytically, we have succeeded in tracing the origin of this discrepancy to an error in earlier work. We provide a thorough treatment of the two-term epsilon expansion, as well as a complete three-dimensional analysis of the fluctuating order-parameter and transverse hydrodynamic modes. The study of the interactions of these modes is carried out to high order so as to arrive at $z_\eta = 0.0679 \pm 0.0007$ for comparison with the experimentally observed value, 0.0690 ± 0.0006.

DOI: 10.1103/PhysRevE.71.021201 PACS number(s): 05.70.Jk, 51.20.+d, 62.10.+s, 64.60.Ht

I. INTRODUCTION

A. General critical behavior

In understanding the critical temperature dependence near the critical point of some extended physical system that is undergoing a second order phase transition, it is essential to adopt a "microscopic" framework. That is, one has to develop an appreciation for the thermally activated fluctuations that are occurring constantly and locally at every point in the medium. In the present work, the fluctuations are those of a scalar order parameter and, on the other hand, the Brownian-motion-type transverse hydrodynamic modes in a fluid. It is the latter which lead to an interesting divergence in the transport properties of the fluid—in particular, of the viscosity studied in this paper. But in order to emphasize the basic origin of such divergences, consider a simpler system, that of interacting spins having a local density of, say, $m(\vec{x}_1)$. Apply a magnetic field H concentrated at point $\vec{x}_1$ and consider the resulting influence on m $(\vec{x}_2)$ at distance $r=|x_2-x_1|$. Because of the interactions between neighboring spins, the thermal average of m $(\vec{x}_2)$ no longer averages to zero but is given by $H\langle m(\vec{x}_1)m(\vec{x}_2)\rangle$, the angular brackets denoting the equilibrium average. Thus the total magnetization, the average value of $\int d^3\vec{x}_2 m(x_2)$, becomes $M=H\int d^3x_2\langle m(\vec{x}_1)m(\vec{x}_2)\rangle$. With the correlation function proportional to $r^{-1-\eta}$ for $r \leqslant \xi$, where ξ is the correlation length, and zero for $r>\xi$, the $r^{-1-\eta}$ for $r \leqslant \xi$, where ξ is the correlation length, and zero for $r>\xi$, the magnetization is $M=HX$, with the susceptibility $X \propto \xi^{2-\eta}$. The correlation length exhibits the critical temperature dependence $(T-T_c)^{-\nu}$, where T_c is the temperature T at the critical point. This yields for the susceptibility the critical exponent $\gamma=(2-\eta)\nu$.

Turning now to the more complicated problem of the interaction in a fluid of the fluctuations of the order-parameter and hydrodynamic modes, we again see the essential role of the correlation length. It dominates the behavior of the long wavelength fluctuations so that the relaxation rate of wave number k is expressed, by $\gamma_\psi(k)=a_\lambda k^{d+z_\eta}$. Here d is the geometric dimensionality of the system and z_η is the critical viscosity exponent, in the sense that the temperature dependence will be expressed by $\xi^{z_\eta} \propto (T-T_c)^{-\nu z_\eta}$, by the dynamic scaling rule of the replacement of k by ξ^{-1} in the long wavelength limit, $k \to 0$. Similarly, the relaxation rate of the hydrodynamic mode has the wave number dependence $\gamma_j = a_\eta k^{2-z_\eta}$. Without the contribution in the exponent of z_η this would reduce to the normal k^2 dependence in the case of a noncritical viscosity. The critical viscosity exponent is thus to be identified with z_η, corresponding to a critical temperature dependence of $\xi^{z_\eta} \propto (T-T_c)^{-\nu z_\eta}$. It is the goal of this paper to calculate the numerical value of z_η. A simple semiqualitative derivation, with a quite minimal account taken of the interactions, is provided below in Eqs. (1.3)–(1.5). To take better into account the interactions, it is necessary to this section, which is a summary of the results obtained in the subsequent sections.

B. Basic concepts of the theory

The framework for the calculation that is set up below in Sec. II is straightforward, but rather complicated in its application. The essential feature is that the interaction of fluctuations which generates the order parameter decay rate, $\gamma_\psi = a_\lambda k^{d+z_\eta}$, is expressed by integrals whose integrands are inversely proportional to a_η. Similarly, the relaxation rate for the hydrodynamic fluctuation of wave number k, $\gamma_j = a_\eta k^{2-z_\eta}$, has integrands inversely proportional to a_η. Multiplying by a_ψ and a_λ, respectively, puts these results into the form of $a_\psi a_\lambda = g_0^2 S_j$ and $a_\psi a_\lambda = g_0^2 S_j$, where g_0^2 is a nonuniversal factor and S_ψ and S_j are certain sums of integrals. It turns

*Present address: Indian Association for the Cultivation of Science, Jadavpur, Calcutta 700032, India.

out that the combination $G \equiv g_0^2/a_\psi a_\lambda$ times the factors $(2\pi)^{-d}$ and C_d (the surface area of a d-dimensional unit sphere) is universal in that it does not depend upon the particular molecular properties of a fluid. This yields for the self-consistent pair of equations $1=Q_\varphi$ and $1=Q_j$. These quantities have expansions of the form shown below in Eqs. (1.10) and (1.11) and contain parametrically the sought-for critical exponent z_η. The search for the numerical value of z_η which satisfies the self-consistency, is facilitated by the fact that the integrals in Q_j are dominated by "divergent-type" parts proportional to z_η^{-1}.

C. Survey of the calculation

In this paper, we present a computation of the critical exponent z_η for the viscosity of a fluid near its critical point. The calculation applies to a one-component fluid as well as to a binary liquid, as these systems belong to the same dynamic scaling universality class. They are both described by a scalar $n=1$, fluctuating order parameter. The work on which we are reporting has been carried out over a sustained period of many years, following in the footsteps of the pioneering and path-breaking study by Siggia *et al.* [1]. The subsequent steps in the development of this subject constitute a kind of successive approximations, as reflected in the organization of this paper. This section, a "bare-bones" introduction, proceeds with a summary of what has been accomplished beyond the ϵ expansion of Sec. III, followed by the three-dimensional treatment in Sec. IV, and, finally, the three-loop computation of Sec. V. The latter provides, we believe, a reliable theoretical numerical value of z_η to compare with experiment. A discussion and summary are contained in Sec. VI.

In setting the stage for the computation, it is useful to start with a brief discussion of the off-diagonal element of the stress tensor

$$T_{xy} \propto \partial_x \partial_y \psi. \tag{1.1}$$

This couples to the transverse hydrodynamic modes of the fluid, as a consequence of fluctuations in the scalar $(n=1)$ order parameter ψ. These can be either fluctuations of entropy density or of concentration, as mentioned above. According to Zwanzig [2] the correlation function for T_{xy} determines the viscosity by means of a kind of Kubo formula. Representing schematically the x and y components of the gradient of ψ by $\cos\theta$, and $\sin\theta\cos\phi$, respectively, yields the average for T_{xy}^2, averaged over all directions in d-dimension space, as

$$\langle \cos^2\theta \sin^2\theta \cos^2\phi\rangle_\Omega = \left.\frac{1}{d(d+2)}\right|_{d=3} = \frac{1}{15}. \tag{1.2}$$

That this is a relatively small number is, evidently, a direct consequence of the transversality of the hydrodynamic modes. In view of Eq. (1.2), it is not surprising that the critical viscosity exponent is rather small in comparison with other critical exponents. Bringing in the critical slowing down of the relaxing modes of wave number p yields a logarithmically divergent integral, with infrared cutoff, which we represent here schematically by

$$\frac{8}{\pi^2}\langle \cos^2\theta \sin^2\theta \cos^2\phi\rangle_\Omega \int_{p>\xi^{-1}} \frac{dp}{p} = z_\eta^{(0)} \ln(\xi/\xi_0), \tag{1.3}$$

where ξ is the correlation length and ξ_0 is a constant of atomic size. Exponentiated, this gives

$$z_\eta^{(0)} \ln(\xi/\xi_0) \simeq (\xi/\xi_0)^{z_\eta^{(0)}} - 1, \tag{1.4}$$

with the low-order critical exponent [3]

$$z_\eta^{(0)} = \frac{8}{15\pi^2}. \tag{1.5}$$

The above low-order result represented by Eq. (1.5) is based on the Ornstein-Zernike approximation $\chi_{oz} \propto q^{-2}$, to the Fourier transform of the order-parameter–order-parameter correlation function. The latter needs to be written more correctly as $\chi \propto q^{-2+\eta}$, where the small anomalous dimension critical exponent is

$$\eta = 0.040, \tag{1.6}$$

as predicted theoretically [4] as well as recently established experimentally [5]. In the Ornstein-Zernike approximation the coupling to a hydrodynamic mode of wave number k is expressed by

$$\chi_{oz}^{-1}(q) - \chi_{oz}^{-1}(k-q) = q^2 - |k-q|^2 = -k^2 + 2\boldsymbol{k}\cdot\boldsymbol{q} \simeq 2\boldsymbol{k}\cdot\boldsymbol{q}. \tag{1.7}$$

in the long wavelength limit, $k \to 0$. With $\eta \neq 0$, this becomes, again with $k \to 0$,

$$\begin{aligned}\chi^{-1}(q) - \chi^{-1}(k-q) &= q^{2-\eta} - (k-q)^{2-\eta} \\ &= q^{2-\eta} - q^{2-\eta}\left(1 - \frac{2}{q^2}(\boldsymbol{k}\cdot\boldsymbol{q})\right)^{1-\eta/2} \\ &\simeq (2-\eta) q^{-\eta} \boldsymbol{k}\cdot\boldsymbol{q}.\end{aligned} \tag{1.8}$$

Thus Eq. (1.5) requires two factors of $1-\eta/2$, giving the first order result

$$z_\eta^{(1)} = \left(1 - \frac{\eta}{2}\right)^2 z_\eta^{(0)}. \tag{1.9}$$

Because the factor $q^{-\eta}$ cancels with $q^{2+\eta}$ to leave q^2, the Ornstein-Zernike approximation for the correlation function, we believe that there is no further correction for $\eta \neq 0$ other than that expressed by Eq. (1.9), except for a factor of $1+\eta/2$ in the one-loop self-consistent decay rate that is exhibited below, in Sec. IV.

The effect of the multiple interactions of the stress tensor of Eq. (1.1) with the hydrodynamic mode is described by the Feynman graphs of Fig. 1 of one, two, three, and more loops, and is computed by the corresponding collections of integrals according to the expansion

$$1 = GI_1 - G^2 I_2 + G^3 I_3 - \cdots, \tag{1.10}$$

for the order parameter. The Feynman graph integrals for the hydrodynamic mode have z_η in the denominator and numerators J_1, J_2, J_3,…, so

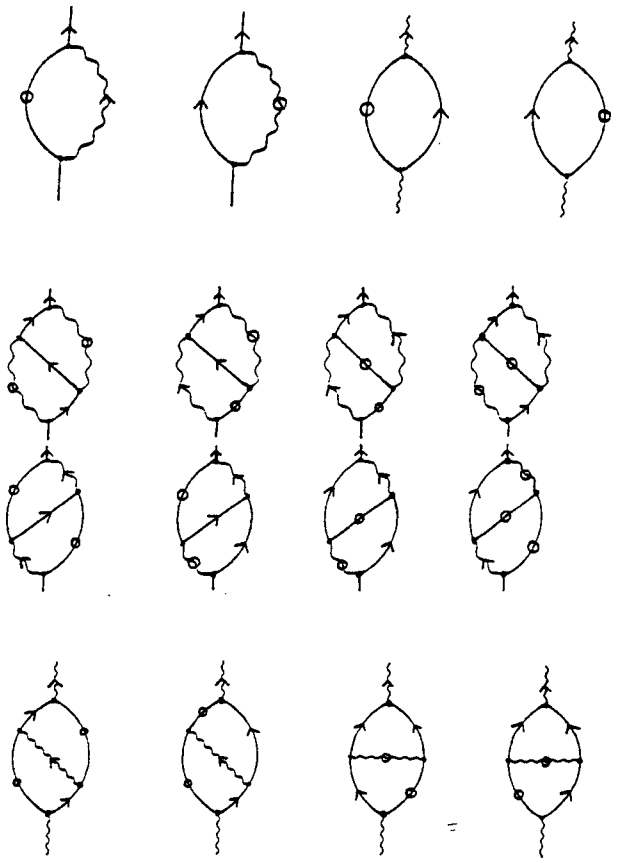

FIG. 1. The one- and two-loop Feynman diagrams for the order-parameter and the hydrodynamic mode decay rates. Solid lines are for the order parameter while wavy lines are for transverse momenta. Lines with circles indicate correlation functions and lines without circles are simply propagators.

$$z_\eta = GJ_1 - G^2J_2 + G^3J_3 - \cdots . \tag{1.11}$$

In these equations, G serves as a kind of coupling constant, the numerical value of which can be determined from Eq. (1.10). At this point an important simplification enters. In the following three sections, it is demonstrated that I_2, the two-loop vertex correction for the order parameter, is quite small compared to I_1, the single loop integral. Furthermore, although the explicit integration for I_1 in Sec. IV does exhibit some small deviation from the bare single-loop value I_{10}, they mutually cancel to have

$$I_1 \simeq I_{10} = \frac{\pi^2}{8}. \tag{1.12}$$

Thus, from the first term of the right hand member of Eq. (1.10), the single-loop approximation to the coupling constant is

$$G = \frac{1}{I_1} \simeq \frac{1}{I_{10}} = \frac{8}{\pi^2}. \tag{1.13}$$

With I_l/I_1 negligibly small for $l \geqslant 3$, we can solve Eq. (1.10) to obtain

$$G = \frac{2}{I_1}\frac{1}{1+(1-4I_2/I_1^2)^{1/2}} \tag{1.14a}$$

which, for $|I_2| \ll I_1^2$, becomes

$$G \simeq I_1^{-1}\left(1+\frac{I_2}{I_1^2}\right). \tag{1.14b}$$

This changes the reference value in Eq. (1.9) for the exponent from $z_\eta^{(1)}$ to

$$\tilde{z}_\eta^{(1)} = \left(1+\frac{I_2}{I_1^2}-\delta\right)z_\eta^{(1)} = \left(1+\frac{I_2}{I_1^2}-\delta\right)\left(1-\frac{\eta}{2}\right)^2 z_\eta^{(0)}, \tag{1.15}$$

where δ is the small nondivergent term in the one-loop integral of Eq. (2.21) below.

With Eq. (1.10) now taken care of, all of our attention and effort has to be directed to Eq. (1.11). The first term of its right hand member yields

$$J_1 = \left(1-\frac{\eta}{2}\right)^2 J_{10} = \left(1-\frac{\eta}{2}\right)^2 \frac{1}{15} \tag{1.16}$$

and

$$z_\eta^{(1)} = GJ_1 = \frac{J_1}{I_1} = \left(1-\frac{\eta}{2}\right)^2 \frac{J_{10}}{I_{10}} = -\left(1-\frac{\eta}{2}\right)^2 z_\eta^{(0)}, \tag{1.17}$$

in agreement with Eqs. (1.5) and (1.9). It is convenient to write Eq. (1.11) as

$$z_\eta^{(1)} = z_\eta^{(1)} F_l, \tag{1.18}$$

where

$$\begin{aligned} F_l &= 1 - G\frac{J_2}{J_1} + G^2\frac{J_3}{J_1} - \cdots \\ &= 1 + G\left|\frac{J_2}{J_1}\right| + G^2\frac{J_3}{J_1} + \cdots + G^l\left|\frac{J_l}{J_1}\right| \end{aligned} \tag{1.19}$$

is an enhancement factor through the lth loop. In Sec. IV, we find, for dimensionality $d=3$,

$$J_2 = -\left(1-\frac{\eta}{2}\right)^2 \frac{1}{45}, \tag{1.20}$$

so

$$G\left|\frac{J_2}{J_1}\right| = \frac{G}{3}. \tag{1.21}$$

The sum over all three-loop graphs in Sec. V yields, again for $d=3$,

$$\left|\frac{J_3}{J_2}\right| = \frac{1}{6}. \tag{1.22}$$

It can be anticipated that this ratio continues for the higher loops, giving

$$F_\infty \simeq 1 + G\left|\frac{J_2}{J_1}\right|\left[1 + \frac{G}{6} + \left(\frac{G}{6}\right)^2 + \cdots\right]$$
$$= 1 + \frac{G}{3}\frac{1}{1 - G/6}$$
$$= \frac{1 + G/6}{1 - G/6}. \quad (1.23)$$

In the discussion and summary of the final section, we employ this result and Eq. (1.15) to obtain a numerical value for z_η.

II. KINETIC EQUATIONS AND PERTURBATION EXPANSION

A. Self-consistent decay rates

Following Kawasaki [6], the kinetic equations that govern the decay of local fluctuations in the order-parameter ψ, the specific entropy, and the transverse momentum density j are

$$\frac{d\psi_k}{dt} = -\frac{\lambda_0 k^2}{\chi_\psi(k)}\psi_k - ig_0\sum_{q,\alpha}(k_\alpha - q_\alpha)j_{q\alpha}\psi_{k-q} + f_{\psi_k} \quad (2.1)$$

and

$$\frac{dj_{k\alpha}}{dt} = -\eta_0 k^2 j_{k\alpha} - ig_0\sum_{q,\beta}\mathcal{T}_{k\alpha\beta}q_\beta\chi_\psi^{-1}(q)\psi_q\psi_{k-q} + f_{j_{k\alpha}}, \quad (2.2)$$

where $\mathcal{T}_{k\alpha\beta} = \delta_{\alpha\beta} - k_\alpha k_\beta/k^2$ is the transverse momentum projection operator and $\chi_\psi(k) = \langle|\psi_k|^2\rangle = 1/k^{2-\eta}$ is the static order-parameter correlation function. Note that the units have been chosen such that $\rho_c = k_B T_c = 1$. In these units, $\chi_j(k) = 1$. The Gaussian noises f_{ψ_k} and $f_{j_{k\alpha}}$ are related to the bare conductivity and λ_0 and η_0 by the fluctuation-dissipation theorems, respectively. The coupling constant g_0 provides the necessary interaction between different modes which, at the critical point, gives rise to the critical divergence.

We want to evaluate the effect of the nonlinear coupling of the modes on the order parameter and transverse momentum relaxation rates, γ_ψ and γ_j. Define, as usual, the correlation functions

$$\langle\psi_k(t)\psi_{-k}(0)\rangle = G_\psi(k,t),$$

and

$$\langle j_{k\alpha}(t)j_{-k\beta}(0)\rangle = \mathcal{T}_{k\alpha\beta}G_j(k,t),$$

for the order parameter ψ and transverse momentum $\mathbf{j}$, respectively. The relaxation rates γ_ψ and γ_j occur explicitly in the frequency Fourier transforms

$$G_\psi(k,\omega) = \frac{\chi_\psi(k)}{-i\omega + \gamma_\psi(k,\omega)}, \quad (2.3)$$

and

$$G_j(k,\omega) = \frac{1}{-i\omega + \gamma_j(k,\omega)}. \quad (2.4)$$

As indicated, γ_ψ and γ_j have both a wave vector $\boldsymbol{k}$ and frequency ω dependence. On the other hand, these correlation functions can also be evaluated in a perturbation expansion from the kinetic equations to obtain

$$\gamma_\psi(k,\omega) = \gamma_\psi^{(0)}(k) + \Sigma(k,\omega) \simeq \Sigma(k,\omega) \quad (2.5)$$

and

$$\gamma_j(k,\omega) = \gamma_j^{(0)}(k) + \prod(k,\omega) \simeq \prod(k,\omega). \quad (2.6)$$

The last steps follow from the fact that the bare relaxation rates $\gamma_\psi^{(0)}(k) = \lambda_0 k^2/\chi_\psi(k)$ and $\gamma_j^{(0)}(k) = \eta_0 k^2$ become unimportant in the long wavelength limit at the critical point. The self-energies become dominant in this regime.

Standard perturbation procedures [7] give these self-energies, in the one-loop order, as

$$\Sigma^{(1)}(k,\omega) = g_0^2\sum_q \frac{\mathbf{k}\cdot\mathcal{T}_q\cdot\mathbf{k}}{\chi_\psi(k)} \times \int_{-\infty}^{\infty}\frac{d\omega'}{2\pi}G_j(q,\omega')G_\psi(k-q,\omega-\omega'), \quad (2.7)$$

and

$$\Pi^{(1)}(k,\omega) = \frac{g_0^2}{2(d-1)}\sum_q \mathbf{q}\cdot\mathcal{T}_k\cdot\mathbf{q}[\chi_\psi^{-1}(q) - \chi_\psi^{-1}(k-q)]^2 \times \int_{-\infty}^{\infty}\frac{d\omega'}{2\pi}G_\psi(q,\omega')G_\psi(k-q,\omega-\omega'), \quad (2.8)$$

where the fully dressed correlation functions are used on the right hand side in order to achieve self-consistency.

The frequency integrations in Eqs. (2.7) and (2.8) are too complicated to perform because the self-consistency condition requires the fully dressed decay rates to be used inside each integrand. Further simplifications are necessary. Introduce the pole approximation [8] for G_ψ as

$$G_\psi^{\mathrm{p}}(k,\omega) = \frac{\chi_\psi(k)}{-i\omega + \gamma_\psi(k)},$$

where $\gamma_\psi(k) = \gamma_\psi(k,\omega=0)$, and similarly for $G_j^{\mathrm{p}}(k,\omega)$. We can write the product $G_\psi G_j$ as

$$G_\psi G_j = [G_\psi^{\mathrm{p}} + (G_\psi - G_\psi^{\mathrm{p}})][G_j^{\mathrm{p}} + (G_j - G_j^{\mathrm{p}})].$$

It was pointed out by Bhattacharjee and Ferrell [9] that the differences are small (order ϵ in the case of ϵ expansion). We can drop the product of two differences when expanding the above expression and get

$$G_\psi G_j \simeq -G_\psi^{\mathrm{p}}G_j^{\mathrm{p}} + G_\psi^{\mathrm{p}}G_j + G_\psi G_j^{\mathrm{p}}.$$

Now the frequency integrations in Eq. (2.7) can be carried out by Cauchy's theorem to yield

$$\frac{1}{2\pi}\int_{-\infty}^{\infty} d\omega' G_j(q,\omega')G_\psi(k-q,\omega-\omega') \simeq \frac{1}{-i\omega+\gamma_\psi(k-q,\omega+i\gamma_j(q))+\gamma_j(q,\omega+i\gamma_\psi(k-q))}.$$

It is generally true that $\gamma_j \gg \gamma_\psi$ near the critical point. Therefore with the omission of γ_ψ in the denominator, the order parameter decay rate, at the self-consistent one-loop order, becomes

$$\gamma_\psi(k,\omega) = g_0^2\chi_\psi^{-1}(k)\int \frac{d^dq}{(2\pi)^d}\mathbf{k}\cdot\mathcal{T}_q\cdot\mathbf{k} \times \frac{\chi_\psi(k-q)}{-i\omega+\gamma_j(q,\omega+i\gamma_\psi(k-q))}. \tag{2.9}$$

Similarly, the same procedure applied to $\gamma_j(k,\omega)$ leads to

$$\gamma_j(k,\omega) = \frac{g_0^2}{2(d-1)}\int \frac{d^dq}{(2\pi)^d}\frac{\boldsymbol{q}\cdot\mathcal{T}_k\cdot\boldsymbol{q}[\chi_\psi^{-1}(q)-\chi_\psi^{-1}(k-q)]^2\chi_\psi(q)\chi_\psi(k-q)}{-i\omega+\gamma_\psi(q,\omega+i\gamma_\psi(k-q))+\gamma_\psi(k-q,\omega+i\gamma_\psi(q))}. \tag{2.10}$$

To close the loop on self-consistency, we need to evaluate the decay rates at the frequency $\omega=i\gamma_\psi(k)$. Note that, in Eq. (2.9), the major contributions to the integration over q come from the large q region. This, together with the fact $\gamma_j \gg \gamma_\psi$, implies that $\gamma_\psi(k,i\gamma_\psi(k)) \simeq \gamma_\psi(k)$. That is,

$$\gamma_\psi(k,i\gamma_\psi(k)) \simeq \gamma_\psi(k) \simeq g_0^2\chi_\psi^{-1}(k)\int \frac{d^dq}{(2\pi)^d}\boldsymbol{k}\cdot\mathcal{T}_q\cdot\boldsymbol{k}\frac{\chi_\psi(k-q)}{\gamma_j(q,i\gamma_\psi(q))}, \tag{2.11}$$

while

$$\gamma_j(k,i\gamma_\psi(k)) = \frac{g_0^2}{2(d-1)}\int \frac{d^dq}{(2\pi)^d}\frac{\boldsymbol{q}\cdot\mathcal{T}_k\cdot\boldsymbol{q}[\chi_\psi^{-1}(q)-\chi_\psi^{-1}(k-q)]^2\chi_\psi(q)\chi_\psi(k-q)}{\gamma_\psi(k)+\gamma_\psi(q)+\gamma_\psi(k-q)}. \tag{2.12}$$

Equations (2.11) and (2.12) form a complete set of self-consistent equations for the order-parameter and transverse momentum decay rates. Although they are evaluated at nonzero frequencies, we can still look for solutions that have the scaling forms required by dynamic scaling, namely

$$\gamma_\psi(k) = a_\lambda k^{4-\eta+z_\lambda} \tag{2.13}$$

and

$$\gamma_j(k,i\gamma_\psi(k)) = a_\eta k^{2-z_\eta}. \tag{2.14}$$

Using the scaling relation [10], $z_\lambda+z_\eta=4-d-\eta$, where d is the spatial dimensionality, we can eliminate z_λ and obtain

$$\gamma_\psi(k) = a_\lambda k^{d+z_\eta}. \tag{2.15}$$

Substituting the above scaling forms for the decay rates into the self-consistent equations, we get, from Eq. (2.11),

$$1 = GI_d^{(1)}(z_\eta), \tag{2.16}$$

where $G=g_0^2C_d/(2\pi)^d a_\lambda a_\eta$, with C_d being the surface area of a d-dimensional unit sphere, and

$$I_d^{(1)}(z_\eta) = \int \frac{d^dq}{C_d}\frac{\sin^2\theta}{q^{2-z_\eta}(k-q)^{2-\eta}}. \tag{2.17}$$

In the above expression, all momenta are scaled by the magnitude of k, making $\mathbf{k}$ itself a unit vector. Similarly, from Eq. (2.12), we obtain

$$1 = GJ_d^{(1)}(z_\eta) \tag{2.18}$$

with

$$J_d^{(1)}(z_\eta) = \frac{1}{2(d-1)} \times \int \frac{d^dq}{C_d}\frac{(q^{2-\eta}-(k-q)^{2-\eta})^2q^2\sin^2\theta}{q^{2-\eta}(k-q)^{2-\eta}[1+q^{d+z_\eta}+(k-q)^{d+z_\eta}]}. \tag{2.19}$$

The integral $I_d^{(1)}(z_\eta)$ can be evaluated in arbitrary dimensionality to yield

$$I_d^{(1)}(z_\eta) = \frac{4}{d-1}\frac{\Gamma(2-z_\eta/2)\Gamma(1-\eta/2)\Gamma(d-1+z_\eta/2+\eta/2)}{\Gamma(d/2)\Gamma(2-d/2-z_\eta/2-\eta/2)\Gamma(d/2-1+z_\eta/2)\Gamma(d/2+z_\eta/2)} \tag{2.20}$$

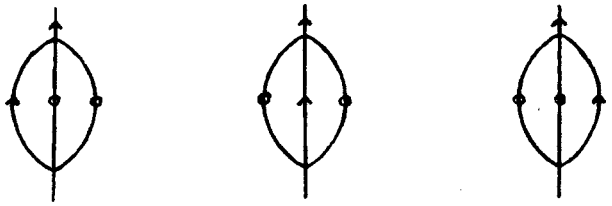

FIG. 2. Two-loop diagrams from the ψ^4 interaction. These diagrams are the first contribution of the ψ^4 coupling to the order-parameter decay rate. A factor of λk^2 is associated with each vertex (with k being the momentum carried by the outgoing propagator from that vertex). In addition, the factor of 6 in Eq. (2.30) is because there are six different ways to construct the diagrams.

and for $J_d^{(1)}(z_\eta)$ we have done an expansion in powers of z_η as

$$J_d^{(1)}(z_\eta) = \frac{J_1}{z_\eta} - \delta, \tag{2.21}$$

where the leading term is found, in the limit of $k \to 0$,

$$J_1 = \left(1 - \frac{\eta}{2}\right)^2 \frac{1}{d(d+2)} \tag{2.22}$$

and the small correction δ as the difference between Eq. (2.19), the complete integral, and the one obtained by taking the $k \to 0$ limit. The exact value of δ depends on dimensionality and will be determined in the next two sections.

B. Two-loop vertex corrections

To estimate the effect of the vertex correction diagrams, one needs to carry out the perturbation expansion to two-loop order. This is a straightforward, though rather tedious, task. Some of the details of this expansion are presented in Appendix A, with others to be found elsewhere [7]. Here we collect the result of this computation. Equations (2.16) and (2.18) are augmented by adding the higher order terms, which are proportional to G^2, to become

$$1 = G I_d^{(1)}(z_\eta) - G^2 I_d^{(v)}(z_\eta) \tag{2.23}$$

and

$$1 = G J_d^{(1)}(z_\eta) - G^2 J_d^{(v)}(z_\eta), \tag{2.24}$$

respectively. $I_d^{(v)}(z_\eta)$ and $J_d^{(v)}(z_\eta)$ correspond to the vertex correction diagrams shown as Figs. 1(d) and 2(c) in Siggia *et al.* [1] and are given by

$$I_d^{(v)}(z_\eta) = \int \frac{d^d p}{C_d} \int \frac{d^d q}{C_d} \frac{[(k-p-q)^{2-\eta} - (k-p)^{2-\eta}][(k-p-q)^{2-\eta} - (k-q)^{2-\eta}]}{(k-p)^{2-\eta}(k-q)^{2-\eta}(k-p-q)^{2-\eta}} \times \frac{[\boldsymbol{k}\cdot\mathcal{T}_p\cdot(\boldsymbol{k}-\boldsymbol{q})][\boldsymbol{k}\cdot\mathcal{T}_q\cdot(\boldsymbol{k}-\boldsymbol{p})]}{p^{2-z_\eta} q^{2-z_\eta}[(k-p)^{d+z_\eta} + (k-q)^{d+z_\eta} + (k-p-q)^{d+z_\eta}]}, \tag{2.25}$$

and

$$J_d^{(v)}(z_\eta) = \frac{1}{d-1} \int \frac{d^d p}{C_d} \int \frac{d^d q}{C_d} \frac{(\boldsymbol{p}\cdot\mathcal{T}_k\cdot\boldsymbol{q})(\boldsymbol{p}\cdot\mathcal{T}_{k-p-q}\cdot\boldsymbol{q})}{(k-p-q)^{2-z_\eta}} \times \frac{p^{2-\eta} - (k-p)^{2-\eta}}{p^{2-\eta}[p^{d+z_\eta} + (k-p)^{d+z_\eta}]} \frac{q^{2-\eta} - (k-q)^{2-\eta}}{q^{2-\eta}[q^{d+z_\eta} + (k-q)^{d+z_\eta}]}. \tag{2.26}$$

Once again, all momenta are scaled by k so that $\boldsymbol{k}$ itself becomes a unit vector.

The leading contribution to $J_d^{(v)}(z_\eta)$ can be evaluated to yield, for arbitrary dimensionality d, as (see Appendix A for more details)

$$J_d^{(v)}(z_\eta) = \frac{J_2}{z_\eta}, \tag{2.27}$$

where

$$J_2 = -\frac{1}{d(d+2)} \frac{1}{d(d-2)}. \tag{2.28}$$

C. Four-point interaction

The last contribution we need to consider at the two-loop level comes from the ψ^4 interaction in the free energy,

$$F = \int d^d r \left(\frac{1}{2}(\nabla\psi)^2 + \frac{r}{2}\psi^2 + \frac{u}{4}\psi^4 \right), \tag{2.29}$$

for the order parameter ψ. To include this interaction, one needs to add an additional term, $\lambda k^2 \Sigma_{p,q} \psi_p \psi_q \psi_{k-p-q}$, to Eq. (2.1). This term's contribution to the order-parameter decay rate comes from the two-loop diagram shown in Fig. 2. The self-energy is then given by

$$\Sigma(k,\omega) = -6u^2\lambda k^2 \sum_{p,q} \chi_\psi(p)\chi_\psi(q)\chi_\psi(k-p-q) \times \frac{\gamma_\psi(p) + \gamma_\psi(q) + \gamma_\psi(k-p-q)}{-i\omega + \gamma_\psi(p) + \gamma_\psi(q) + \gamma_\psi(k-p-q)}. \tag{2.30}$$

The $\omega = 0$ limit of this self-energy is simply the lowest order expression that gives rise to the nonzero anomalous dimension η and thus has been taken into account through the use

of Eq. (1.6). Only the frequency dependent part of this self-energy contributes to the dynamic effects, and it is

$$\delta\Sigma(k,\omega) = \Sigma(k,\omega) - \Sigma(k,0) = -i\omega 6u^2 \gamma_\psi(k)\chi_\psi(k) \times \int \frac{d^d p}{(2\pi)^d} \int \frac{d^d q}{(2\pi)^d} \frac{\chi_\psi(p)\chi_\psi(q)\chi_\psi(k-p-q)}{-i\omega + \gamma_\psi(p) + \gamma_\psi(q) + \gamma_\psi(k-p-q)}, \tag{2.31}$$

where we have replaced λk^2 by $\gamma_\psi(k)\chi_\psi(k)$. Equation (2.3) is then modified to read

$$G_\psi(k,\omega) = \frac{\chi_\psi(k)}{-i\omega + \gamma_\psi(k) + \delta\Sigma(k,\omega)}. \tag{2.32}$$

Using the pole approximation that was introduced earlier, the self-consistent equation for the order-parameter decay rate, Eq. (2.23), becomes

$$1 = \frac{G I_d^{(1)}(z_\eta) - G^2 I_d^{(v)}(z_\eta)}{1 + 6u^2[C_d/(2\pi)^d]^2 K_d(z_\eta)}, \tag{2.33}$$

where

$$K_d(z_\eta) = \int \frac{d^d p}{C_d} \int \frac{d^d q}{C_d} \frac{1}{p^{2-\eta} q^{2-\eta} (k-p-q)^{2-\eta} [1 + p^{d+z_\eta} + q^{d+z_\eta} + (k-p-q)^{d+z_\eta}]}. \tag{2.34}$$

Once again, all momenta are scaled by the external momentum k, making it a unit vector. Having set up all the necessary formalism, we are ready to evaluate the critical exponent z_η next.

III. ϵ EXPANSION

At the one-loop level, it is easy to expand Eq. (2.20) in powers of $\epsilon = 4-d$ to yield, using the static renormalization group value of $\eta = \epsilon^2/54$,

$$I_d^{(1)}(z_\eta) = \frac{3}{4} \frac{1}{\epsilon - z_\eta} \left(1 + \frac{\epsilon}{6} - \frac{z_\eta}{4} + \frac{\eta}{\epsilon - z_\eta}\right) + O(\epsilon), \tag{3.1}$$

where we have kept the first two terms of the expansion. Equation (2.21) can also be expanded easily. But there is still a $O(1)$ term that was left out in the evaluation of the leading contribution. This contribution can be obtained by integrating the difference between the full integral in Eq. (2.19) and the simplified one used in the leading contribution calculation by taking $k \to 0$. Details of this evaluation is left to Appendix A. Here we simply state the result

$$J_d^{(1)}(z_\eta) = \frac{1}{24 z_\eta} \left(1 + \frac{5}{12}\epsilon\right) - \frac{2\ln 2 - 1}{32} + O(\epsilon). \tag{3.2}$$

Substituting these two expression into Eqs. (2.10) and (2.12), z_η is found to be

$$z_\eta = \frac{\epsilon}{19} \left\{1 + \left[\frac{1}{4}\left(1 - \frac{1}{19^2}\right) - \frac{1}{54} - \frac{2\ln 2 - 1}{32} \frac{432}{361}\right]\epsilon + O(\epsilon^2)\right\}$$

$$= \frac{\epsilon}{19}[1 + 0.216\epsilon + O(\epsilon^2)]. \tag{3.3}$$

As a note, we emphasize that the one-loop calculation presented in this section does not make the Markovian assumption and thus has taken proper account of the frequency dependence of the decay rates. Self-consistency is achieved by using nonzero frequencies, thereby significantly simplifying the calculations. It should also be noted that, although Eq. (3.3) gives $z_\eta = 0.064$ when evaluated at $\epsilon = 1$, it is incomplete in the ϵ^2 order. Higher order perturbation expansion, namely the two-loop vertex corrections, also contribute to this order.

Of the two-loop contributions discussed in Sec. II, the four-point interaction contributes only to order ϵ^3 and higher. As a result, only the order-parameter and transverse momentum vertex corrections need to be included and Eqs. (2.23) and (2.24) are sufficient.

The evaluations of Eqs. (2.25) and (2.26) are made simpler in the ϵ expansion, since both diverge logarithmically at $d=4$ and we only need the leading $O(1/\epsilon)$ terms. We can therefore neglect the unit vector k in comparison with p and q wherever possible. As a result, all the remaining $\boldsymbol{k}$ dependencies are in the numerators of each integrand, affording an averaging over all $\boldsymbol{k}$ directions. The leading divergence can then be picked out by scaling one momentum, say q, by the other and by carrying out the integration over p. The remaining integrations can then be performed entirely analytically for $d=4$ with no necessity for any numerical evaluation. The result that follows from the discussion in Appendix A is

$$I_d^{(v)}(z_\eta) = -\frac{8\ln 2 - 5}{64} \frac{1}{\epsilon - z_\eta} + O(1), \tag{3.4}$$

and, from Eqs. (2.27) and (2.28),

$$J_d^{(v)}(z_\eta) = -\frac{1}{192 z_\eta} + O(1). \tag{3.5}$$

The corresponding vertex correction integrals of Siggia *et al.* [1], namely Eqs. (A16) (A21), differ from our Eqs. (2.25) and (2.26) only by a factor of 2. Therefore it is appropriate to compare our result, Eqs. (2.27) and (2.28), with theirs. Tak-

ing into account the factor 2, which is due to the difference in the definition of the coupling constant, we see that the numerical constant for $J_d^{(v)}$ is identical with that in Eq. A22 of Siggia *et al.* However, our numerical value for the coefficient in $I_d^{(v)}(z_\eta)$, $(8\ln 2-5)/64=0.008\,52$, is ten times smaller [11] than that given by Eq. A17 of Siggia *et al.* With this correction to $I_d^{(v)}(z_\eta)$, these two vertex corrections will no longer cancel each other in the final result. Instead, only $J_d^{(v)}$ makes a significant contribution with $I_d^{(v)}$ playing a minor role. This vertex correction for the order parameter has less than 0.5% effect on the viscosity exponent, as seen below in Eq. (3.7). The incorrect value of $I_d^{(v)}$ used by Siggia *et al.* resulted in a spurious reduction of z_η by 10%.

Substituting Eqs. (3.4) and (3.5) into Eq. (2.23), we get for G

$$G=\frac{4}{3}(\epsilon-z_\eta)\left(1-\frac{\epsilon}{6}+\frac{z_\eta}{4}\right)-\frac{4}{3}\eta-\frac{4}{3}\left(\frac{24}{19}\right)^2\frac{8\ln 2-5}{64}\epsilon^2+O(\epsilon^3) \tag{3.6}$$

and for the viscosity exponent

$$z_\eta=\frac{\epsilon}{19}\left\{1+\left[\frac{1}{4}\left(1-\frac{1}{19^2}\right)-\frac{1}{54}-\frac{2\ln 2-1}{32}\frac{432}{361}+\frac{3}{32}\left(\frac{24}{19}\right)^2-\frac{8\ln 2-5}{64}\left(\frac{24}{19}\right)^2\right]\epsilon+O(\epsilon^2)\right\}$$

$$=\frac{\epsilon}{19}[1+0.352\epsilon+O(\epsilon^2)]. \tag{3.7}$$

In the first line of this equation, the contributions from each source are kept separate for easy identification. The discussion and comparison of these results with our earlier one-loop ones as well as others are provided in the following section. Finally, putting z_η back into Eq. (3.6), we find for the constant G

$$G=\frac{24}{19}\epsilon-0.247\epsilon^2+O(\epsilon^2). \tag{3.8}$$

Another critical exponent, that for the thermal conductivity λ, can be obtained from the scaling relation $z_\lambda+z_\eta=\epsilon-\eta$. The result is

$$z_\lambda=\frac{18}{19}\epsilon[1-0.039\epsilon+O(\epsilon^2)]. \tag{3.9}$$

A further quantity of interest is the universal amplitude R in the Stokes-Einstein relation

$$D=\frac{\lambda}{c_p}=\frac{Rk_BT}{6\pi\eta\xi^{d-2}}. \tag{3.10}$$

In the units that we have been working with, i.e., $\rho_c=k_BT_c=1$, we get, by substituting the asymptotic forms of λ and η

$$R=6\pi a_\lambda a_\eta=6\pi\frac{C_d}{(2\pi)^d}\frac{1}{G}. \tag{3.11}$$

Using the ϵ expansion for G found earlier at the end of previous section, we find for R

$$R=\frac{3}{\pi}\frac{19}{24\epsilon}[1+0.196\epsilon+O(\epsilon^2)]. \tag{3.12}$$

For three-dimensional space, we substitute $\epsilon=1$ and get $z_\eta=0.071$ and $R=0.90$. Some inadequacies of the ϵ expansion have been discussed in detail by Bhattacharjee and Ferrell [12] who argued that a loop expansion was more appropriate. They also showed the necessity to solve the self-consistent coupled mode equations in three dimensions in order to obtain a more precise result. The following section presents the result of this three-dimensional calculation.

IV. VISCOSITY EXPONENT IN THREE DIMENSIONS

Unlike in the ϵ expansion of the previous section, the integrals $J_d^{(1)}(z_\eta)$ and others will have to be calculated numerically in three dimensions. The only exceptions is $I_d^{(1)}\times(z_\eta)$ which can be evaluated exactly for arbitrary dimensionality as shown in Eq. (2.20). For $d=3$, we can expand $I_d^{(1)}(z_\eta)$ in powers of the small exponents η and z_η. It turns out that the linear terms in z_η cancel each other out, leaving only the simple first order expression,

$$I_3^{(1)}(z_\eta)=I_1\simeq\frac{\pi^2}{8}\left(1+\frac{\eta}{2}\right)=\left(1+\frac{\eta}{2}\right)I_{10}, \tag{4.1}$$

where $I_{10}=\pi^2/8$ is the single-loop order parameter integral for $\eta=0$. The order-parameter vertex correction $I_3^{(v)}(z_\eta)$ is now a convergent integral and is found numerically to have the small value

$$I_3^{(v)}=I_2\simeq 0.0052. \tag{4.2}$$

For the transverse momentum decay rate, the one-loop as well as the two-loop vertex correction diagrams have their leading contributions proportional to $1/z_\eta$ as shown by Eqs. (2.21) and (2.28) of Sec. II. In addition to the leading contributions, we will also need to estimate the first correction for $J_3^{(1)}$. This is done numerically by evaluating the difference, with the small exponent z_η set to zero, between the full expression, as given by Eq. (2.19), and the simplified $k\to 0$ one used in the calculation of the leading contribution. The latter is given by Eq. (2.21),

$$J_1=\left(1-\frac{\eta}{2}\right)^2\frac{1}{15}, \tag{4.3}$$

when evaluated at $d=3$, and the value for the first correction is found to be

$$\delta=0.954\times 10^{-2} \tag{4.4}$$

For the transverse momentum vertex correction, we only need the leading contribution as given by Eq. (2.28), evaluated at $d=3$,

$$J_3^{(v)}(z_\eta)=\frac{J_2}{z_\eta}, \tag{4.5}$$

where

$$J_2 = -\left(1-\frac{\eta}{2}\right)^2 \frac{1}{45} = \frac{J_1}{3}. \tag{4.6}$$

Similar to the one-loop integral $J_3^{(1)}$, the first correction to Eq. (4.5) is a constant term. Computation of this nondivergent term is difficult. Its magnitude, similarly to Eq. (4.4), can be estimated as $z_\eta \delta \simeq 7\times 10^{-4}$ and thus negligible in the subsequent work.

The final remaining integral is $K_d(z_\eta)$. For this term, we will use the static renormalization group result for the fixed point value of u, in an ϵ expansion,

$$u = \frac{8\pi^2\epsilon}{(n+8)^2}. \tag{4.7}$$

At three dimensions, $\epsilon=1$. Since this u is from an ϵ expansion, we will evaluate $K_d(0)$ in $d=4$. This was done numerically to yield

$$K_4(0) = \int \frac{d^4p}{C_4}\int \frac{d^q}{C_4}\frac{1}{p^2q^2(k-p-q)^2[1+p^4+q^4+(k-p-q)^4]} = \frac{2}{\pi^2}1.2996 \pm 0.0006. \tag{4.8}$$

Putting these results together, Eq. (2.26) becomes

$$1 + K = GI_3^{(1)} - G^2 I_3^{(v)}, \tag{4.9}$$

where $K=6u^2[C_4/(2\pi)^4]^2K_4(0)=0.0195$. Since both $I_3^{(v)}$ and K are small, we can solve this equation for G as

$$G \simeq \frac{1+K}{I_1}\left(1+\frac{I_2}{I_1^2}\right) = \frac{1+K}{1+\eta/2}I_{10}^{-1}\left(1+\frac{I_2}{I_1^2}\right) \simeq I_{10}^{-1}\left(1+\frac{I_2}{I_1^2}\right), \tag{4.10}$$

so the small effect here of K is canceled to better than 0.1% accuracy by the substitution of $\eta=0.04$ into Eq. (4.10). Substituting Eq. (4.10) into Eq. (2.24) yields for the critical viscosity exponent,

$$(1+G\delta)z_\eta^{(2)} = GJ_1 - G^2J_2 = GJ_1F_2, \tag{4.11}$$

where

$$F_2 = 1 - G\frac{J_2}{J_1} = 1 + \frac{G}{3} = 1 + \frac{1}{3I_{10}} = 1.270 \tag{4.12}$$

is a kind of two-loop enhancement factor. From the insertion of Eq. (4.4), the remaining factors in Eq. (4.11) are

$$GJ_1 = \left(1+\frac{I_2}{I_1^2}\right)\left(1-\frac{\eta}{2}\right)^2\frac{J_{10}}{I_{10}} \simeq \left(1+\frac{I_2}{I_1^2}\right)(1-\eta)z_\eta^{(1)}, \tag{4.13}$$

where we recognize

$$z_\eta^{(1)} = \frac{J_{10}}{I_{10}} = \frac{8}{15\pi^2} = 0.0540, \tag{4.14}$$

as the lowest order single-loop approximation. The final result of the computation is therefore, to two-loop order,

$$z_\eta^{(2)} \simeq \frac{1+I_2/I_1^2}{1+G\delta}(1-\eta)F_2 z_\eta^{(1)} = 1.214 z_\eta^{(1)} = 0.0656. \tag{4.15}$$

V. THREE-LOOP VERTEX CORRECTIONS

In the preceeding sections, we showed that the transverse momentum vertex correction diagrams have the greatest contributions to the value of z_η among all the two-loop contributions. To estimate the higher order effect, let us concentrate on the three-loop transverse momentum vertex correction diagrams.

These three-loop vertex correction diagrams for the transverse momentum can be grouped into three general types. Figure 3 shows one representative diagram from each type. For the diagram shown in Fig. 3(a), there is a total of 18 different variations [13]. It is a straightforward, but tedious, exercise to show that the sum of these 18 diagrams gives

$$\delta\gamma_\psi^{(3)} = \frac{1}{d-1}\int\frac{d^dp}{(2\pi)^d}\int\frac{d^dq}{(2\pi)^d}\int\frac{d^dr}{(2\pi)^d}\left(1-\frac{\chi_\psi(p)}{\chi_\psi(k-p)}\right)\left(1-\frac{\chi_\psi(r)}{\chi_\psi(k-r)}\right)\frac{\chi_\psi(q)}{\chi_\psi(k-q)}$$
$$\times \frac{\boldsymbol{p}\cdot\mathcal{T}_k\cdot\boldsymbol{r}(\boldsymbol{k}-\boldsymbol{q})\cdot\mathcal{T}_{p-q}\cdot\boldsymbol{q}(\boldsymbol{k}-\boldsymbol{r})\cdot\mathcal{T}_{q-r}\cdot\boldsymbol{r}}{\gamma_j(p-q)\gamma_j(q-r)[\gamma_\psi(p)+\gamma_\psi(k-p)][\gamma_\psi(q)+\gamma_\psi(k-q)][\gamma_\psi(r)+\gamma_\psi(k-r)]}. \tag{5.1}$$

The contributions from the other two types of diagrams, Figs. 3(b) and 3(c), can be shown to be small when compared with

the first type. To illustrate this point, consider the frequency integrals involved in a typical diagram represented by Fig. 3(b), which can be written as

$$\int \frac{d\omega'}{2\pi}\int \frac{d\omega''}{2\pi}\int \frac{d\omega'''}{2\pi}\frac{1}{-i\omega'+\chi_\psi(p)}\frac{1}{-i(\omega-\omega')+\gamma_\psi(k-p)}\times\frac{1}{-i\omega'''+\chi_\psi(r)}\frac{1}{-i(\omega-\omega''')+\gamma_\psi(k-r)}$$
$$\times\frac{1}{-i\omega''+\chi_\psi(q)}\frac{1}{-i(\omega-\omega'+\omega''-\omega''')+\gamma_\psi(k-p+q-r)}\times\frac{1}{-i(\omega'-\omega'')+\chi_j(p-q)}\frac{1}{-i(\omega''-\omega''')+\gamma_j(q-r)}$$
$$\simeq\frac{1}{-i\omega+\gamma_\psi(p)+\gamma_\psi(k-p)}\frac{1}{-i\omega+\gamma_\psi(r)+\gamma_\psi(k-r)}\times\frac{1}{-i\omega+\gamma_j(p-q)}\frac{1}{\gamma_j(p-q)[\gamma_j(p-q)+\gamma_j(q-r)]}. \tag{5.2}$$

Compare Eq. (5.2) with Eq. (5.1); a factor of γ_j has replaced γ_ψ in Eq. (5.1). Since $\gamma_j \gg \gamma_\psi$, the contributions from this type of diagram should be much smaller than those from Fig. 3(a). Intuitively, this is so because the crossed transverse momentum propagators force one of the middle two order-parameter propagators to their time scale, which is much shorter. A similar argument can be made for diagrams represented by Fig. 3(c).

Having established that the only important three-loop contributions are contained in Eq. (5.1), we go back to evaluate them. Substituting the scaling relations, it is trivial to show that

$$J_d^{(3)}=\frac{1}{d-1}\int\frac{d^dp}{C_d}\int\frac{d^dq}{C_d}\int\frac{d^dr}{C_d}\left(1-\frac{(k-p)^{2-\eta}}{p^{2-\eta}}\right)\left(1-\frac{(k-r)^{2-\eta}}{r^{2-\eta}}\right)$$
$$\times\frac{q^{2-\eta}}{(k-q)^{2-\eta}}\frac{\boldsymbol{p}\cdot\mathcal{T}_k\cdot\boldsymbol{r}(\boldsymbol{k}-\boldsymbol{q})\cdot\mathcal{T}_{q-p}\cdot\boldsymbol{q}(\boldsymbol{k}-\boldsymbol{r})\cdot\mathcal{T}_{q-r}\cdot\boldsymbol{r}}{(p-q)^{2-z}{}_\eta(q-r)^{2-z}{}_\eta}\times\frac{1}{[p^{d+z}{}_\eta+(k-q)^{d+z}{}_\eta][q^{d+z}{}_\eta+(k-q)^{d+z}{}_\eta][r^{d+z}{}_\eta+(k-r)^{d+z}{}_\eta]}, \tag{5.3}$$

where $\boldsymbol{k}$ is a unit vector. As with the lower order transverse momentum diagrams, the leading divergent part can be obtained by expanding the integrand in powers of $\boldsymbol{k}$. Keeping only the lowest order in the expansion and then averaging over all directions of $\boldsymbol{k}$, we obtain

$$J_d^{(3)}(z_\eta)=\frac{(1-\eta/2)^2}{2(d-1)}\int\frac{d^dp}{C_d}\int\frac{d^dq}{C_d}\int\frac{d^dr}{C_d}\frac{d(\boldsymbol{p}\cdot\boldsymbol{r})^2-p^2r^2}{p^2r^2}$$
$$\times\frac{\boldsymbol{q}\cdot\mathcal{T}_{p+q}\cdot\boldsymbol{q}\boldsymbol{r}\cdot\mathcal{T}_{q+r}\cdot\boldsymbol{r}}{(p+q)^{2-z}{}_\eta(q+r)^{2-z}{}_\eta p^{d+z}{}_\eta q^{d+z}{}_\eta r^{d+z}{}_\eta} \tag{5.4}$$

where we have changed $\boldsymbol{q}$ to $-\boldsymbol{q}$ in order to make it easier to evaluate the integrals later. If we define $\boldsymbol{p}\cdot\boldsymbol{q}=pq\cos(\theta)$, $\boldsymbol{q}\cdot\boldsymbol{r}=qr\cos(\theta')$ and $\boldsymbol{p}\cdot\boldsymbol{r}=pr\cos(\theta'')$, and scale both $\boldsymbol{p}$ and $\boldsymbol{r}$ by q, we can integrate over $\boldsymbol{q}$, with a lower cutoff limit of 1 to obtain the leading contribution as

$$J_d^{(3)}(z_\eta)=\frac{(1-\eta/2)^2}{2(d-1)}\frac{1}{z_\eta}\int\frac{d^d\Omega_p}{C_d}$$
$$\times\sin^2\theta\int_0^\infty\frac{pdp}{[1+2p\cos(\theta)+p^2]^2}$$
$$\times\int\frac{d^d\Omega_r}{C_d}(d\cos^2\theta''-1)$$
$$\times\sin^2\theta'\int_0^\infty\frac{rdr}{(1+2r\cos\theta'+r^2)^2}. \tag{5.5}$$

The integrals can be performed similarly to those in $J_d^{(v)}$ (see Appendix A) to yield

$$J_d^{(3)}(z_\eta)=\frac{J_3}{z_\eta}, \tag{5.6}$$

where

$$J_3=\left(1-\frac{\eta}{2}\right)^2\frac{1}{d(d+2)}\frac{1}{2d^2(d-2)^2}=\frac{J_2}{2d(d-2)}, \tag{5.7}$$

which is the value for J_3 used in Eq. (1.22) when evaluated at $d=3$.

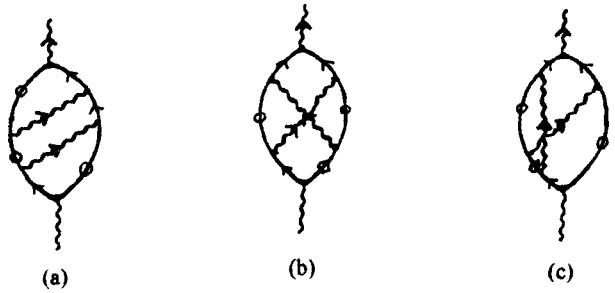

FIG. 3. Typical three-loop diagrams for the transverse momentum modes. Diagrams of the types (b) and (c) can be shown to be small as compared with the contributions from (a).

VI. DISCUSSION AND CONCLUSIONS

The ϵ-expansion calculation of the critical viscosity exponent, $z_\eta=0.0071$, is largely the result of underestimating the one-loop order-parameter decay rate as shown in Fig. 4 [12] by the way of 30% smaller value of $I_d^{(1)}$ in three dimensions.

The three dimensional one-loop coupled-mode result of $z_\eta = 8/15\pi^2 = 0.0054$ also cannot be regarded as a correct prediction because of the contributions from the higher loops. The inclusion, as a first step, of the two-loop effects requires the vertex correction diagrams, as well as the ψ^4 interaction. However, the order-parameter decay rate is not significantly changed by the addition of its vertex correction term because of the smallness of $I_3^{(v)}$, as shown in Eq. (4.2). Furthermore, the contributions to the order-parameter decay rate from the ψ^4 interaction almost cancel each other as evidenced by Eq. (4.10). Substituting Eq. (4.2), the value of $I_3^{(v)}$, into Eq. (4.10), we obtain, for the coupling constant G in $d=3$,

$$G = 0.8133. \tag{6.1}$$

Of all the two-loop contributions, it is the transverse momentum vertex corrections that contribute most significantly to the final value of z_η.

The two-loop treatment of the critical viscosity exponent demonstrates that the two-loop order-parameter vertex correction is negligibly small and causes us to adopt a general rule according to which it is permitted to neglect as well the higher order graphs in this category. This leaves the three-loop graphs for the vertex correction of the viscous mode, which we evaluated in the previous section and found to be $\frac{1}{6}$ of that from the two-loop graphs. If we assume that the higher order contributions for the viscous mode continue with the same ratio, the enhancement factor F_∞ of Eq. (1.23) can easily be obtained using Eq. (6.1) as

$$F_\infty = 1.3136. \tag{6.2}$$

Equation (4.11) can easily be extended to include the three-loop and higher effects as

$$z_\eta^{(\infty)} = GJ_1F_\infty/(1 + G\delta), \tag{6.3}$$

which gives the final value for z_η to be

$$z_\eta = z_\eta^{(\infty)} = 0.0679 \pm 0.0007. \tag{6.4}$$

For comparison purposes, if we stop at the three-loop, the value for the enhance factor is $F_3 = 1.3078$ and the value of critical viscosity exponent is $z_\eta^{(3)} = 0.0676$, which is only slightly smaller than the value of $z_\eta^{(\infty)}$. The final result of the theory effort [14], as expressed by Eq. (6.4), can be compared to the experimentally measured critical exponent, 0.0690 ± 0.0006, as reported by Berg *et al.* [15].

ACKNOWLEDGMENTS

We would like to acknowledge helpful discussions with Dr. R. F. Berg, Dr. M. R. Moldover, and Professor J. V. Sengers. This work was supported by the National Aeronautics and Space Administration via Grant for Basic Research No. NAG 3-1867.

APPENDIX A

We provide, in this appendix, some details for evaluating the integrals $I_d^{(v)}$ and $J_d^{(v)}$. Consider first the simpler of the two, $J_d^{(v)}$. In the limit of $z_\eta = 0$, simple power counting shows that it is logarithmically divergent. As a result, we can expand the numerator in powers of k and neglect it in comparison with p and q in the demoninator. From Eq. (2.26), we obtain

$$J_d^{(v)}(z_\eta) \simeq \frac{(1 - \eta/2)^2}{d-1} \times \int \frac{d^dp}{C_d} \int \frac{d^dq}{C_d} \frac{\boldsymbol{p}\cdot\mathcal{T}_k\cdot\boldsymbol{qp}\cdot\mathcal{T}_{p+q}\cdot\boldsymbol{qp}\cdot\boldsymbol{kk}\cdot\boldsymbol{q}}{p^{2+d+z_\eta}q^{2+d+z_\eta}(p+q)^{2-z_\eta}}. \tag{A1}$$

Averaging the above over all directions of $\mathbf{k}$, we get

$$\langle(\boldsymbol{p}\cdot\boldsymbol{k}\,\boldsymbol{k}\cdot\boldsymbol{q})(\boldsymbol{p}\cdot\mathcal{T}_k\cdot\boldsymbol{q})\rangle = \frac{p^2q^2}{d(d+2)}(d\cos^2\theta - 1), \tag{A2}$$

where θ is the angle between $\boldsymbol{p}$ and $\boldsymbol{q}$. The other angular dependent factor $\boldsymbol{p}\cdot\mathcal{T}_{p+q}\cdot\boldsymbol{q}$ can also be simplified to

$$\boldsymbol{p}\cdot\mathcal{T}_{p+q}\cdot\boldsymbol{q} = \boldsymbol{p}\cdot\boldsymbol{q} - \frac{\boldsymbol{p}\cdot(\boldsymbol{p}+\boldsymbol{q})(\boldsymbol{p}+\boldsymbol{q})\cdot\boldsymbol{q}}{(p+q)^2} = -\frac{p^2q^2\sin^2\theta}{(p+q)^2}. \tag{A3}$$

$J_d^{(v)}(z_\eta)$ then becomes

$$J_d^{(v)}(z_\eta) = -\frac{1}{d(d+2)}\frac{1}{d-1} \times \int \frac{d^dp}{C_d} \int \frac{d^dq}{C_d} \frac{p^2q^2(d\cos^2\theta - 1)\sin^2\theta}{(p+q)^{4-z_\eta}p^{d+z_\eta}q^{d+z_\eta}}. \tag{A4}$$

If we scale q by p so that $\boldsymbol{l} = \boldsymbol{q}/p$, the integration over p can then carried out with a lower cutoff of 1 for p to yield

$$J_d^{(v)}(z_\eta) \simeq -\frac{1}{d(d+2)}\frac{1}{d-1}\frac{1}{z_\eta}\int \frac{d^dl}{C_d}\frac{l^2(d\cos^2\theta - 1)\sin^2\theta}{(1 + 2l\cos\theta + l^2)^2 l^d}, \tag{A5}$$

where we have neglected z_η in the remaining integral since the leading $1/z_\eta$ behavior has already been captured by the integration over p. The integration over the radial direction of l can be carried out first since

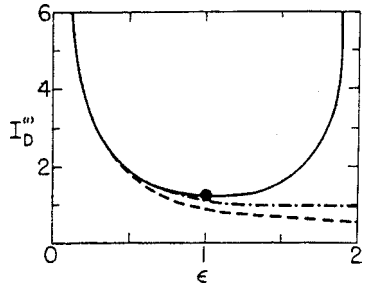

FIG. 4. One-loop integral $I_d^{(1)}$ vs $\epsilon = 4 - d$, where d is the spatial dimensionality. Solid curve shows the exact function [Eq. (2.20) with z_η and η set to zero] with value of $I_{10} = \pi^2/8$ indicated by the solid dot. The 30% error of the two-term ϵ expansion by Siggia *et al.* [1] is shown by the dashed curve.

$$\int_0^\infty \frac{ldl}{(1+2l\cos\theta+l^2)^2} = \frac{1}{2\sin^3\theta}(\sin\theta - \theta\cos\theta). \tag{A6}$$

The remaining integrations over θ are elementary and can be obtained easily to yield Eqs. (2.27) and (2.28).

The evaluation of $I_d^{(v)}(z_\eta)$ follows a similar line when performed as an ϵ expansion because it has the same logarithmic divergence at $d=4$. By neglecting k in the denominator, we can average over all directions of k in the numerator to obtain

$$\langle \boldsymbol{k}\cdot\mathcal{T}_p\cdot(\boldsymbol{k}-\boldsymbol{q})\boldsymbol{k}\cdot\mathcal{T}_q\cdot(\boldsymbol{k}-\boldsymbol{p})\rangle = -\frac{pq}{d}\cos\theta\sin^2\theta, \tag{A7}$$

where θ is again the angle between $\boldsymbol{p}$ and $\boldsymbol{q}$. $I_d^{(v)}(z_\eta)$ then becomes

$$I_d^{(v)}(z_\eta) = -\frac{1}{d}\int\frac{d^dp}{C_d}\int\frac{d^dq}{C_d}\frac{pq\cos\theta\sin^2\theta[(p+q)^2-p^2][(p+q)^2-q^2]}{p^{4-z_\eta}q^{4-z_\eta}(p+q)^2[p^{d+z_\eta}+q^{d+z_\eta}+(p+q)^{d+z_\eta}]} + O(1). \tag{A8}$$

Once again, we can integrate over one momentum, say p, by introducing $\boldsymbol{l}=\boldsymbol{q}/p$ to obtain

$$I_d^{(v)}(z_\eta) = -\frac{1}{\epsilon - z_\eta}\frac{1}{\pi}\int_0^1 dl\int_0^\pi d\theta\frac{l\cos\theta\sin^4\theta(l+2\cos\theta)(1+2l\cos\theta)}{(1+2l\cos\theta+l^2)[1+l^4+(1+2l\cos\theta+l^2)^2]} + O(1). \tag{A9}$$

The integrand can be separated, using partial fraction, into simpler terms as

$$\frac{l\cos\theta\sin^4\theta(l+2\cos\theta)(1+2l\cos\theta)}{(1+2l\cos\theta+l^2)[1+l^4+(l+2l\cos\theta+l^2)^2]}$$
$$= A + B\cos\theta + C\cos^2\theta + D\cos^3\theta + E\cos^4\theta + \frac{F}{1+2l\cos\theta+l^2} + \frac{G+H\cos\theta}{1+l^4+[1+2l\cos\theta+l^2)^2]}, \tag{A10}$$

where the coefficients $A-H$ are functions of l only. The integration over θ are familiar with the possible exception of the last term in Eq. (A10) which can be evaluated using

$$\int_0^\pi d\theta\frac{1}{1+l^4+(1+2l\cos\theta+l^2)^2} = \frac{\pi}{2}\frac{1+l^2}{1+l^2+l^4}\frac{1}{\sqrt{1+l^4}}, \tag{A11}$$

and

$$\int_0^\pi d\theta\frac{\cos\theta}{1+l^4+(1+2l\cos\theta+l^2)^2} = -\frac{\pi}{2}\frac{l}{1+l^2+l^4}\frac{1}{\sqrt{1+l^4}}. \tag{A12}$$

The remaining integration over l is tedious but straightforward. In the end, we arrived at Eq. (3.4).

[1] E. D. Siggia, B. I. Halperin, and P. C. Hohenberg, Phys. Rev. B **13**, 2110 (1976).
[2] J. M. Deutch and R. Zwanzig, J. Chem. Phys. **46**, 1612 (1967).
[3] R. A. Ferrell, Phys. Rev. Lett. **24**, 1169 (1970); R. Perl and R. A. Ferrell, Phys. Rev. A **6**, 2358 (1972).
[4] R. A. Ferrell and J. K. Bhattacharjee, Phys. Rev. Lett. **42**, 1505 (1979).
[5] A. Lytle and D. T. Jacobs, J. Chem. Phys. **120**, 5709 (2004).
[6] K. Kawasaki, Ann. Phys. (N.Y.) **61**, 1 (1970); T. Ohta and K. Kawasaki, Prog. Theor. Phys. **55**, 1384 (1976).
[7] H. Hao, Ph.D. thesis, University of Maryland, 1991.
[8] R. A. Ferrell and J. K. Bhattacharjee, J. Low Temp. Phys. **36**, 165 (1979).
[9] J. K. Bhattacharjee and R. A. Ferrell, Phys. Rev. A **23**, 1511 (1981); **27**, 1544 (1983).
[10] P. C. Hohenberg and B. I. Halperin, Rev. Mod. Phys. **49**, 435 (1977).
[11] After our work had been finished, we learned that L. Peliti had also detected this error by means of a numerical integration, P. C. Hohenberg (private communication).
[12] J. K. Bhattacharjee and R. A. Ferrell, Phys. Rev. A **28**, 2363 (1983).
[13] P. Das and J. K. Bhattacharjee, Phys. Rev. E **67**, 036103 (2003).
[14] It needs to be noted that the computations leading to Eq. (6.4) are based on neglecting the nondivergent parts of the vortex corrections, which are presumed to be small enough to be negligible. This question continues to be under investigation.
[15] R. Berg, M. L. Moldover, and G. A. Zimmerli, Phys. Rev. E **60**, 4079 (1999).